The Mechanism of Heat Transfer in a Spray Column Heat Exchanger

RUTH LETAN and EPHRAIM KEHAT

Technion, Israel Institute of Technology, Haifa, Israel

Temperature profiles of dispersed kerosene and water were measured in a spray column heat exchanger, 15 cm. in diameter and 160 cm. long. Dispersed packing of drops and narrow temperature ranges were used. The flow rates used were 0 to 50 liters/min. of water and 5 to 40 liters/min. of kerosene. The physical picture that emerges from the temperature profiles is that heat is transferred from fully mixed drops to fully mixed wakes while the wakes are formed, by shedding and renewal of elements of wakes in most of the column and by complete mixing of all streams at the water inlet at the top of the column. Mathematical equations were developed from the physical model. The volume of the wakes and the rate of shedding of wake elements were estimated from the temperature profiles and were used to calculate the temperature profiles for this and for other studies. The agreement of the calculated profiles with the experimental data is very good.

A spray column heat exchanger system is composed of two spray columns. In one column heat is transferred by direct contact from hot water to a countercurrent flow of cold oil. In the other column the heated oil transfers heat to cold water. This type of heat exchanger has been suggested for use in desalination schemes (*23*, *32*). The favorable features of a spray column heat exchanger are simplicity, low cost, high heat throughput, and no scale deposition on heat transfer surfaces. An attempt to scale up a spray column heat exchanger from a laboratory sized column failed (*30*).

In most studies of heat transfer in single spray columns (*1* to 3, *7*, *9*, *12*, *15*, *26*, *27*, *30*, *32*) only inlet and outlet temperatures of the two streams were measured. Plug flow and ideal countercurrent heat transfer were assumed, and log mean temperature differences were used to calculate volume heat transfer coefficients or values of HTU. This large amount of data cannot be correlated to give the quantitative effects of the many parameters involved.

The temperature profiles of the continuous phase were measured by Pierce et al. (*24*) for short columns and by Letan and Kehat (*16*) for a longer column. The development of a method to trap and measure the temperature of flowing drops (*17*) made possible the measurement of the temperature profiles of both phases in this work. About 200 temperature profiles were measured. The temperature profiles showed, consistently, the following features (Figures 8 to 12): At the bottom of the column the drops temperature changed rapidly while the continuous phase temperature remained constant. At face value this appears to violate the conservation of energy. This is the key evidence for the role of the wakes of drops in the mechanism of heat transfer. In this region both drop and wake experience a rapid temperature change, while the continuous phase temperature remains constant. A short region with no temperature change of both phases (at low holdups only) followed. Higher up the column the temperature of the two phases changed continuously, with a small temperature difference between them. At the top of the column a sharp temperature jump of the continuous phase at its inlet took place and all streams leaving that region were at the same temperature. These observations confirm earlier suggestions of the role played by the wakes of drops in the mechanism of heat or mass transfer in a spray column (*6*, *16*) and of a mixing process that takes place at the top of the column (*16*).

Some studies (*5*, *6*, *10*, *31*) have shown that most of the mass transfer to or from drops takes place on the downstream side of the drops. Very little is known about the formation and shedding of wakes of liquid drops. Magarvey and Bishop (*19*, *20*) studied the shapes of

Ephraim Kehat is Visiting Associate Professor, Purdue University, Lafayette, Indiana.

shed wakes of drops and the frequency of wake shedding for a wide range of Reynolds numbers. Hendrix et al. (*11*) measured the volume of wakes of drops under non-oscillating or oscillating conditions. The range of the Reynolds number in this work (based on drop diameter, slip velocity and water density and viscosity) was 40 to 1,000. For single spheres the formation of wakes starts at Reynolds numbers of 8 to 24 (*19, 22, 29*) while wake shedding starts at Reynolds numbers of the order of 200 to 500 (*19, 21, 29*). Collision with other drops probably encourages wake shedding at lower Reynolds numbers.

THE PHYSICAL MODEL

A detailed visualization of the physical model and the general form of the temperature profiles are shown in Figure 1. An earlier paper (*16*) proposed a physical model of heat transfer in a spray column. It is now possible to give a more detailed description of the mechanism of heat transfer in the five zones shown in Figure 1. For convenience, cooling drops rising in a spray column heat exchanger are described.

Wake Growth Zone *a*

The drop is formed by the breakup of a liquid jet of the dispersed phase in the continuous phase. After the drop travels a short distance, separation of the boundary layer takes place on the downstream part of the drop. A toroidal vortex is formed and grows and the separation ring moves forward. At the separation point disturbances are created which gives rise to turbulent motion in the continuous phase close to the boundary. This results in greatly enhanced drop to wake heat transfer (*31*). Oscillations of the drop start and a high degree of turbulent mixing takes place inside the drops (*25*). The boundary layer at the separation ring is still at the temperature of the continuous phase because conduction and convection upstream of the drop are relatively small (*6*). The elements of the separated boundary layer move in vortices at the bottom of the drop and reach the temperature of the surface of the drop due to the low resistance to heat transfer in that region. These elements enter the highly mixed vortices of the wake and stay there till the wake attains its maximum volume. All this time the wake accumulates all the heat lost by the drop and the average temperature of the wake is higher than the average temperature of the drop. Conduction of heat from the wake to the continuous phase is negligible, compared with the heat transferred by the shed elements of wakes, higher up the column. In this region the drop and its wake rise through a low population of drops.

Intermediate Zone *b*

The drop continues to rise and enters a denser region of drops (*18*). Random collisions with other drops take place. The frequency of oscillations of the drop and the wake increases considerably with increased number of collisions and increased proximation of other drops. No temperature change takes place in this zone. At the top of this zone the wake starts to expel elements of its substance from the vortex ring.

Wake Shedding Zone *c*

The flow rate of the continuous phase into the wake through the boundary layer equals the flow rate of the continuous phase expelled from the wake. The elements of the continuous phase, reach the boundary separation ring still at the continuous phase local temperature. They are heated to the drop temperature in the vortex region behind the drop and enter the highly mixed wake. The elements of the continuous phase leaving the wake are at the mixed wake temperature. The amounts of material entering and leaving the wake are small, relative to its size. The temperatures of the drops, wakes and continuous phase decrease gradually up the column.

Mixing Zone *d*

All streams, drops, wakes, incoming continuous phase and returning wakes from the coalescence zone enter this

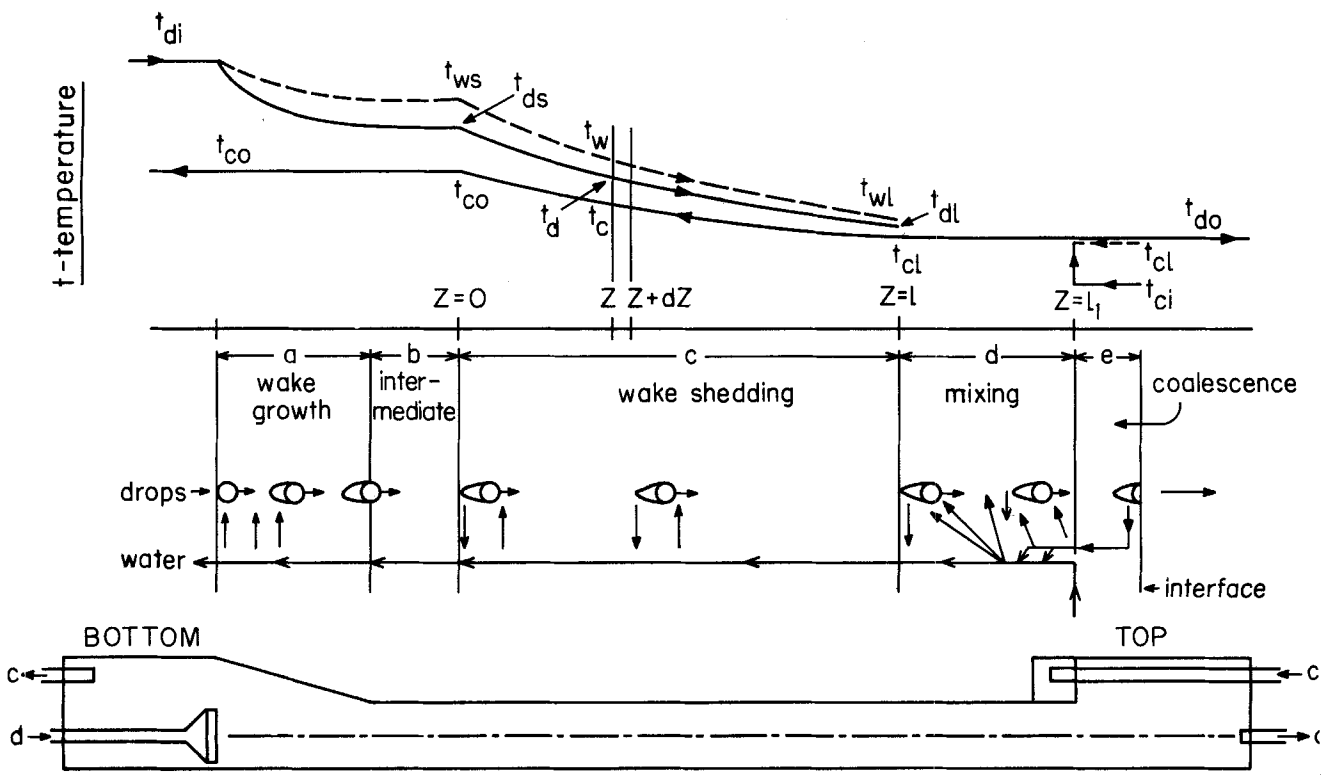

Fig. 1. Physical model of heat transfer in a spray column heat exchanger.

highly mixed zone and leave at the same temperature (t_{cl}).

Coalescence Zone e

The drop approaches the upper interface and coalesces with the liquid above the interface. At the interface the wake is completely detached from the drop and flows back down the column together with the entering stream of the continuous phase. Practically no heat transfer takes place in this zone.

THE MATHEMATICAL MODEL

Heat transfer takes place only in zones *a*, *c* and *d*. The following assumptions are made:

Steady state, no heat losses, constant average physical properties of the liquids, constant average holdup, constant average drop size, the final wake volume is constant, the flow rates in and out of the wake are equal in zone *c*.

In zone *a* the drop is fully mixed. Elements of the continuous phase reach the temperature of the drop and then enter the fully mixed wake. Heat balance on the drop (Figure 2) gives:

$$(\rho Cp)_c\,(t_{co} - t_d)\,dM_D = v_D\,(\rho Cp)_d\,dt_d \qquad (1)$$

Integration of Equation (1) for the whole zone results in

$$M = r \ln \frac{t_{di} - t_{co}}{t_{ds} - t_{co}} \qquad (2)$$

where

$$r = \frac{(\rho Cp)_d}{(\rho Cp)_c} \qquad (3)$$

From Equation (2) we get

$$t_{ds} = (t_{di} - t_{co}) \exp\left(-\frac{M}{r}\right) + t_{co} \qquad (4)$$

The temperature of the wake at the top of this zone (t_{ws}) can be calculated from an overall heat balance:

$$M_D\,(\rho Cp)_c\,(t_{ws} - t_{co}) = v_D\,(\rho Cp)_d\,(t_{di} - t_{ds}) \qquad (5)$$

If we eliminate t_{ds} by the use of Equation (4) we obtain

$$t_{ws} = \frac{r}{M}(t_{di} - t_{co})\left[1 - \exp\left(-\frac{M}{r}\right)\right] + t_{co} \qquad (6)$$

In zone *b* no heat transfer takes place in this zone and $t_d = t_{ds}$, $t_w = t_{ws}$ and $t_c = t_{co}$ at $z = 0$, the point at the onset of shedding.

In zone *c* heat balance on the drop (Figure 3*a*) gives

$$(\rho Cp)_c\,(t_c - t_d)\,dm_w = v_D\,(\rho Cp)_d\,dt_d \qquad (7)$$

Division by dz gives

$$\frac{dt_d}{dz} + \frac{m}{r}(t_d - t_c) = 0 \qquad (8)$$

where by the last assumption

$$m = \frac{1}{v_D}\frac{dm_w}{dz} \qquad (9)$$

Heat balance on the wake (Figure 3*a*) gives

$$(\rho Cp)_c\,(t_d - t_w)\,dm_w = M_D\,(\rho Cp)_c\,dt_w \qquad (10)$$

When we divide by dz we obtain

$$\frac{dt_w}{dz} + \frac{m}{M}(t_w - t_d) = 0 \qquad (11)$$

Heat balance on the continuous phase (Figure 3*b*) takes into account the total stream of the continuous phase, including the wakes that return from the coalescence zone (MV_d).

$$(V_c + MV_d)\,(\rho Cp)_c\,dt_c = V_d\,(\rho Cp)_c(t_c - t_w)\frac{dm_w}{v_D} \qquad (12)$$

Division by dz gives

$$\frac{dt_c}{dz} + \frac{m}{P}(t_w - t_c) = 0 \qquad (13)$$

where

$$P = \frac{V_c + MV_d}{V_d} = \frac{1}{R} + M \qquad (14)$$

and

$$R = V_d/V_c \qquad (15)$$

Equations (8), (11), and (13) can be solved simultaneously with the boundary conditions at $z = 0$: $t_d = t_{ds}$, $t_w = t_{ws}$, $t_c = t_{co}$.

Equations (4) and (6) were used to replace t_{ds} and t_{ws} in terms of t_{di} and t_{co}. The resulting temperatures of the drops, the continuous phase and the wakes as function of z are given in a dimensionless form in Equations (16) to (18) following:

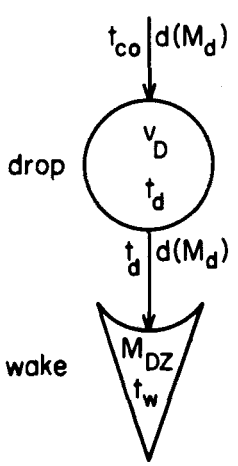

Fig. 2. Heat transfer in the wake formation zone.

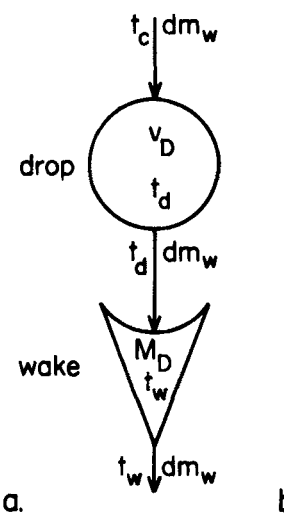

Fig. 3. Heat transfer in the wake shedding zone a—drop and wake b—continuous phase.

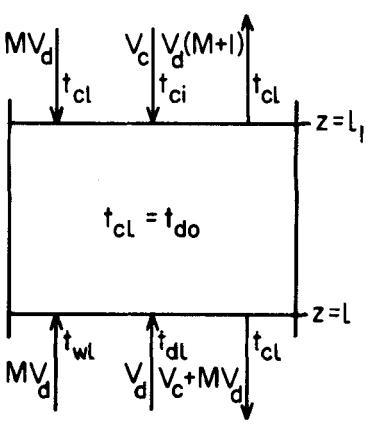

Fig. 4. Heat transfer in the mixing zone.

$$\theta_d = \frac{t_d - t_{co}}{t_{di} - t_{co}} = \left\{ \frac{m}{r} \left[\frac{1+S}{\alpha_1} [1 - \exp(a_1 z)] - \frac{S}{\alpha_2} [1 - \exp(\alpha_2 z)] \right] + 1 \right\} \exp\left(-\frac{M}{r}\right) \quad (16)$$

$$\theta_c = \frac{t_c - t_{co}}{t_{di} - t_{co}} = \left\{ \frac{m}{r} \left[\frac{1+S}{\alpha_1} \left[1 - \left(\frac{r}{m}\alpha_1 + 1\right) \exp(\alpha_1 z) \right] - \frac{S}{\alpha_2} \left[1 - \left(\frac{r}{m}\alpha_2 + 1\right) \exp(\alpha_2 z) \right] \right] + 1 \right\} \exp\left(-\frac{M}{r}\right) \quad (17)$$

$$\theta_w = \frac{t_w - t_{co}}{t_{di} - t_{co}} = \left\{ \frac{m}{r} \left[\frac{1+S}{\alpha_1} \left[1 - \left(\frac{r}{m}\alpha_1 + 1\right) \left(1 - \frac{P}{m}\alpha_1\right) \exp(\alpha_1 z) \right] - \frac{S}{\alpha_2} \left[1 - \left(\frac{r}{m}\alpha_2 + 1\right) \left(1 - \frac{P}{m}\alpha_2\right) \exp(\alpha_2 z) \right] \right] + 1 \right\} \exp\left(-\frac{M}{r}\right) \quad (18)$$

where

$$\alpha_{1,2} = -\frac{m}{2} \left[\left(\frac{1}{M} + \frac{1}{r} - \frac{1}{P}\right) \pm \sqrt{\left(\frac{1}{M} + \frac{1}{r} + \frac{1}{P}\right)^2 - \frac{4}{Mr}} \right]$$

$$S = \frac{\alpha_1 + \frac{m}{r} - \frac{r\,m}{P\,M}\left[\exp\left(\frac{M}{r}\right) - 1\right]}{\alpha_2 - \alpha_1} \quad (19)$$

In zone d heat balance on the whole zone (Figure 4) gives

$$MV_d (\rho Cp)_c t_{wl} + V_d (\rho Cp)_d t_{dl} + V_c (\rho Cp)_c t_{ci} = [(V_c + MV_d)(\rho Cp)_c + V_d (\rho Cp)_d] t_{cl} \quad (20)$$

which can be written as

$$t_{ci} = [R(r + M) + 1] t_{do} - R(r t_{dl} + M t_{wl}) \quad (21)$$

since

$$t_{do} = t_{cl} \quad (22)$$

to give the temperature at the inlet of the continuous phase. This temperature can also be calculated from an overall heat balance around the whole column. This is written as

$$V_d (\rho Cp)_d (t_{di} - t_{do}) = V_c (\rho Cp)_c (t_{co} - t_{ci}) \quad (23)$$

to give

$$t_{ci} = t_{co} - Rr (t_{di} - t_{do}) \quad (24)$$

Equations (16), (17), (22) and (24) and specified temperatures at the bottom of the column, make possible the calculation of the temperature profiles of the two phases in the column.

THE TEMPERATURE APPROACH AT THE ENDS OF THE COLUMN

For optimum utility, close temperature approach between the two phases at both ends of the column is desired. Limitation by the specifications and an economic analysis will determine the practical temperature approach. The effect of the values of the parameter Rr, for very long columns on the temperature approach are discussed in this section.

At the top of the wake shedding zone b analysis of Equation (19) can easily show that

$$\alpha_1 < 0, \quad S < 0 \quad (25)$$

and that

$$\begin{aligned} \alpha_2 &> 0 \quad \text{for } Rr > 1 \\ \alpha_2 &= 0 \quad \text{for } Rr = 1 \\ \alpha_2 &< 0 \quad \text{for } Rr < 1 \end{aligned} \quad (26)$$

The temperature approach at the top of the wake shedding zone can be obtained from Equations (16) and (17) for $t_d = t_{dl}$ and $t = t_{cl}$ at $z = l$, in the form:

$$\Delta\theta_l = \frac{t_{dl} - t_{cl}}{t_{di} - t_{co}} = [(1 + S)\exp(\alpha_1 l) - S\exp(\alpha_2 l)] \exp\left(-\frac{M}{r}\right) \quad (27)$$

For long enough columns and $Rr < 1$, the exponential terms will be small since both α_1 and α_2 have negative values and

$$\Delta\theta_l = 0 \quad (28)$$

For long enough columns and $Rr = 1$, $\alpha_2 = 0$ and

$$\Delta\theta_l = -S\exp\left(-\frac{M}{r}\right) \quad (29)$$

a small positive value.

For long enough columns and $Rr > 1$, $\alpha_2 > 0$ and

$$\Delta\theta_l \to \infty \quad (30)$$

Obviously for a close temperature approach, values of $Rr \leq 1$ are required. It will be shown that for long enough columns and $Rr \leq 1$ the temperature jump is zero and therefore a close temperature approach can be obtained at the top of the column.

The temperature jump ratio (θ_a) is defined by

$$\theta_a = \frac{t_{cl} - t_{ci}}{t_{co} - t_{ci}} \quad (31)$$

By the introduction of t_{cl} from Equation (17) for $t_c = t_{cl}$ at $z = 1$, $t_{cl} = t_{do}$ from Equation (22), and t_{ci} from Equation (24) we obtain

$$\theta_a = 1 - \frac{1}{Rr\left(1 - \frac{1}{F}\right)} \quad (32)$$

where

$$F = \left\{ \frac{m}{r} \left(\frac{1+S}{\alpha_1} \left[1 - \left(\frac{r}{m}\alpha_1 + 1\right) \exp(\alpha_1 l) \right] - \frac{S}{\alpha_2} \left[1 - \left(\frac{r}{m}\alpha_2 + 1\right) \exp(\alpha_2 l) \right] \right) + 1 \right\} \exp\left(-\frac{M}{r}\right) \quad (33)$$

For long enough columns and $Rr < 1$, Equation (33) reduces to:

$$F = \left[\frac{m}{r} \left(\frac{1+S}{\alpha_1} - \frac{S}{\alpha_2} \right) + 1 \right] \exp\left(-\frac{M}{r}\right) \quad (34)$$

Combination of Equations (27), (28), (31) and (34) yields

$$\theta_a = 0 \quad (35)$$

For long enough columns and $Rr = 1$ Equation (33) reduces to

$$F \to \infty \quad (36)$$

Combination of Equations (32) and (36) for $Rr = 1$ yields

$$\theta_a = 0 \quad (37)$$

For long enough columns and $Rr > 1$, Equation (33) reduces to

$$F \to \infty \tag{38}$$

Combination of Equations (32) and (38) for $Rr > 1$ yields

$$\theta_a \to 1 - \frac{1}{Rr} > 0 \tag{39}$$

Here again values of $Rr \leq 1$ are desirable for close temperature approach. Equation (24) can be rearranged in the form

$$Rr = \frac{t_{co} - t_{ci}}{t_{di} - t_{do}} \tag{40}$$

If a close temperature approach is obtained at the top of the column and $t_{do} - t_{ci} = \epsilon$, a small value, then at the bottom of the column, we obtain

$$\begin{array}{lll} \text{for} & Rr < 1 & t_{di} - t_{co} > \epsilon \\ \text{for} & Rr = 1 & t_{di} - t_{co} = \epsilon \\ \text{for} & Rr > 1 & t_{di} - t_{co} < \epsilon \end{array} \tag{41}$$

For close temperature approach values of $Rr \geq 1$ are desirable. As a result of Equations (28) to (30), (35), (37), (39), and (41) the best value of Rr is $Rr = 1$.

EXPERIMENTAL PROCEDURE

The experimental column 1 in Figure 5 was made of Pyrex, 15 cm. in diameter and 160 cm. long. The distance between the inlets of the two streams was 195 cm. Tanks 2 and 3 contained steam coils, cooling water coils, electrical heaters and thermostats. Constant flow conditions and constant location of the upper interface were maintained by controlling the flows to and out of the column at the same rates by valves 18 to 25 and readings of matched pairs of rotameters, 10 to 17. At low flow rates constant head tanks 6 and 7 and two pairs of lower range rotameters were used. At high flow rates the two liquids were fed by the pumps 8 and 9 to the column through two pairs of higher range rotameters. The materials of construction were mainly aluminum and chrome plated brass. The whole system was insulated by rockwool. The sections of inlet pipes inside the column were also insulated. The dispersion plate contained a calming section and one hundred thirty 4 cm. long, 1.5 mm. I.D. stainless steel needles, arranged in concentric circles.

The dispersed liquid was kerosene and the continuous liquid was distilled water. Both liquids were mutually saturated. The range of flow rates was 5 to 40 liter/min. of kerosene and 0 to 50 liter/min. of water. All runs were made with a dispersed packing of drops. The average drop size was 3.3 to 3.55 mm. in most runs and the average holdup was 0.06 to 0.56. The dynamic behavior of the column had been studied earlier (*18*) and the average holdup and holdup distribution for the whole range of operation were known.

The temperature profiles were measured by means of 32-30 gauge copper constantan thermocouples. Four thermocouples were located at the inlets anl outlets of the streams and fourteen pairs of thermocouples were located at the center along the column. The positions of the thermocouples are shown in Figures 8 to 12. One thermocouple of each pair measured the local water temperature and the other one, that was located in the center of a polythylene bed (*17*) that was wet by the kerosene, measured the kerosene drops temperature at that location. The thermocouples calibration was checked in air and water every ten runs. The accuracy of the thermocouples readings was ± 0.05°C. In all runs the temperature difference between incoming streams was about 10°C. in order to minimize effects of varying physical properties of the systems with temperature. Three series of runs were made at an average temperature of 35°C. for cooling and for heating drops, and at an average temperature of 65°C. for cooling drops. About two hundred runs were made of which about fifty were duplicates. Temperatures were recorded only after all thermocouples gave steady state readings. A heat balance was made for each run. In most cases runs for which the heat transferred by both streams varied by more than 10% were discarded.

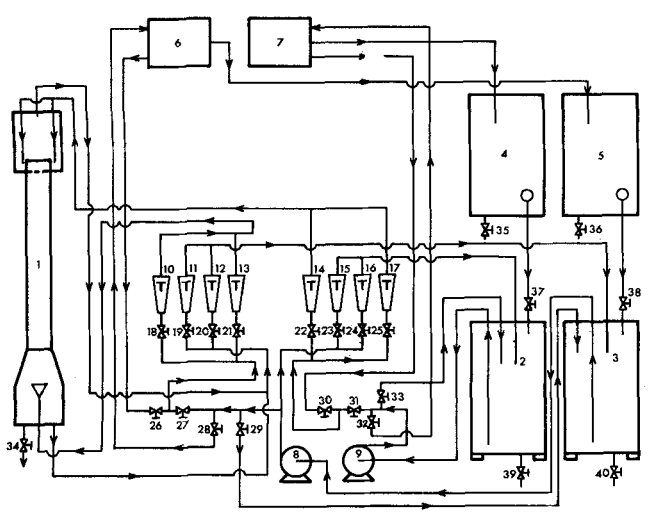

Fig. 5. Flow sheet of the experimental system.

RESULTS

Typical temperature profiles are shown in Figures 8 to 12. The length of the wake shedding zone, which is the major part of the column, can be calculated from the theoretical model, for any desired heat throughput, once the parameters M and m have been determined. The lengths of the other zones were determined experimentally from the temperature profiles. The results are summarized in Table 1. At higher holdups for spray columns with a conical entry section, the drop packing extends into the conical entry section and the effective length of the drop packing is larger than the length of the column proper by l'. The values of l' which are a function of the flow rates of the two phases are also given in Table 1.

The values of the wake volume per drop volume (M) were calculated from the temperature profiles for the wake growth zone by Equation (2).

$$M = r \ln \frac{t_{di} - t_{co}}{t_{ds} - t_{co}}$$

The values of M were correlated with the average holdup in the intermediate zone (H_b), which was calculated by integration of the holdup profiles for each run.

Table 1. The Lengths of Zones *a*, *b*, *d*, *e* and the Extension of Drop Packing into the Conical Entry Section.

Zone	Length, cm	Remarks
Wake growth, a	$Z_a = 0$ to 35	decreases with increased holdup
Intermediate, b	$Z_b = 42 - 100\,H_b$	for $0.06 \leq H_b \leq 0.42$
	$Z_b = 0$	for $H_b > 0.42$
Mixing, d	$Z_d < 60$	increases with increased R
	$Z_d = 0$	for $R \to 0$
Coalescence, e	Z_e = controllable	depends on location of upper interface
Extension of drop packing into conical entry section	$l' = 0$	for $H < 0.20$
	$l' = 10$ to 30	for $0.30 < H < 0.60$

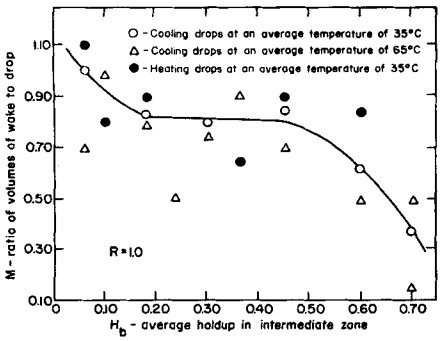

Fig. 6. Ratio of wake to drop volumes as function of the average holdup in the intermediate zone.

The holdup in this zone probably has an effect on the value of M and is more sensitive to the effect of variation of R than the average holdup in the column. The holdup in this zone can be higher than the average holdup of the column. At high holdups, where the intermediate zone did not exist, the point value at $z = 0$ was used.

The results are shown in Figure 6. The correlating curve was drawn only for cooling drops at an average temperature of 35°C. This was the most reliable set of data with the best heat balance. However no significant effects of the higher temperature or the change in direction of heat flow were noted. At holdups of 0.15 to 0.45 M is about 0.83. At lower holdups M is somewhat higher and decreases at higher holdups, as can be expected from the interference of neighboring drops. These values of M are of the order of magnitude of wake sizes measured by Taneda (*29*) for solid spheres. The correlation suggested by Hendrix et al. (*11*) based on wake sizes of smaller, nonoscillating drops yields values of M an order of magnitude higher, which seem excessive.

The amount of wake elements shed per drop volume and unit length of column (m), was calculated by means of Equation (8) which can be rearranged in the form

$$m = r\frac{-dt_d/dz}{t_d - t_c} \qquad (42)$$

Values of m were calculated from the measured temperature profiles, at $z = 0$, for the runs at $R = 1$. The data show considerable scatter since slopes of smoothed curves between point measurements were measured. The values of m as a function of the point holdup at $z = 0$ are shown in Figure 7. These values range between 0.01 and 0.04. The correlating curve was drawn only for cooling drops at an average temperature of 35°C. as in Figure 6. Experience in calculating temperature profiles showed that the useful representative range is between 0.023 and 0.03.

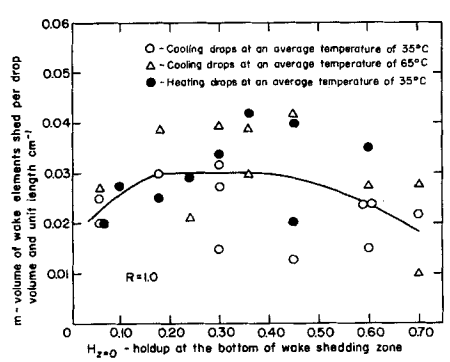

Fig. 7. Elements of wake shed per drop volume and unit length of column as function of the holdup at $z = 0$.

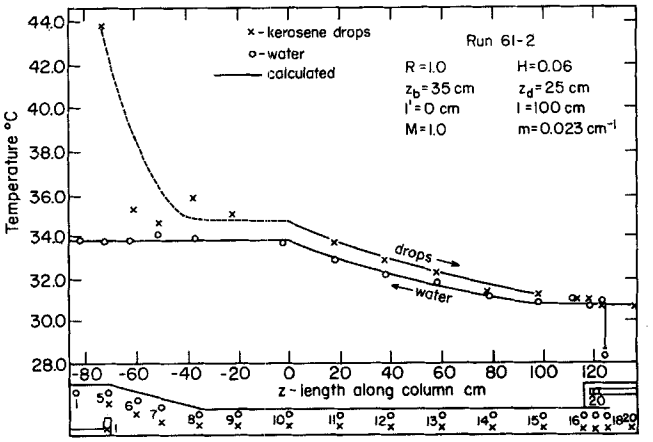

Fig. 8. Experimental and calculated temperature profiles of water and kerosene for cooling drops and an average temperature of 35°C., for $R = 1.0$ and $H = 0.06$.

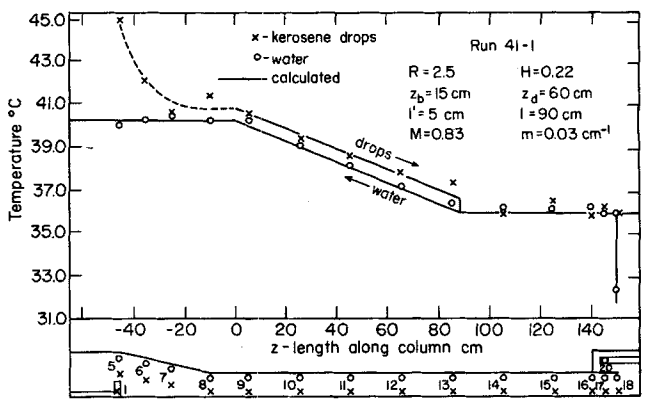

Fig. 9. Experimental and calculated temperature profiles of water and kerosene for cooling drops and average temperature of 35°C., for $R = 2.5$ and $H = 0.22$.

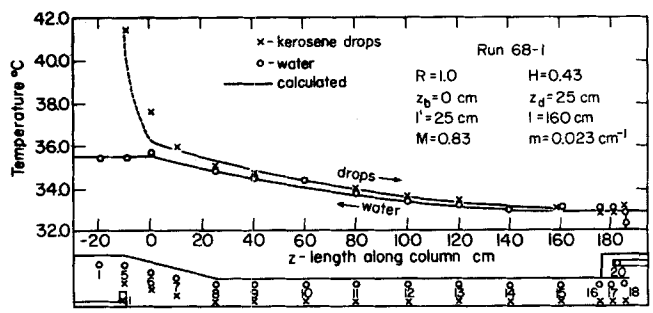

Fig. 10. Experimental and calculated temperature profiles of water and kerosene for cooling drops and average temperature of 35°C., for $R = 1.0$ and $H = 0.43$.

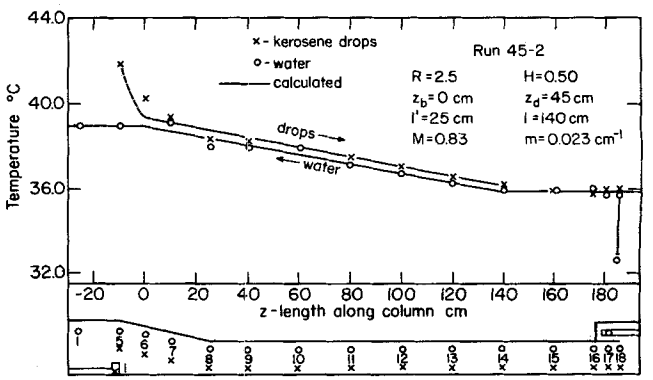

Fig. 11. Experimental and calculated temperature profiles of water and kerosene for cooling drops and average temperature of 35°C., for $R = 2.5$ and $H = 0.50$.

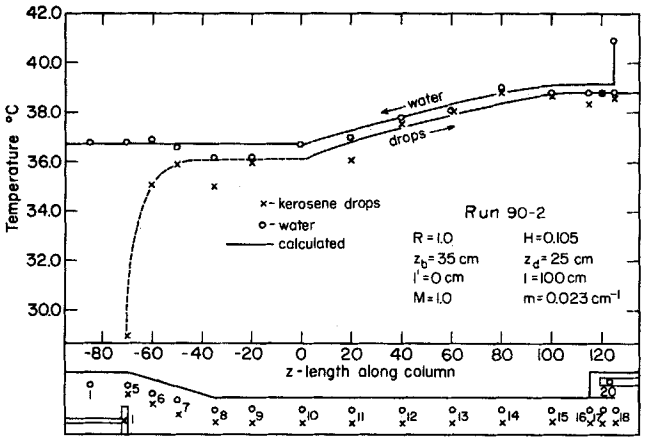

Fig. 12. Experimental and calculated temperature profiles of water and kerosene for heating drops and average temperature of 35°C., for $R = 1.0$ and $H = 0.105$.

VERIFICATION OF THE THEORETICAL MODEL

Equations (16), (17), (22), and (24) and the data of Table 1 and Figures 6 and 7 make possible the calculation of the temperature profiles. The values of M and m used in these calculations are given in Table 2.

At low holdups, the holdup is constant along the column, and experimental values of M and m can be used. At higher holdups, the holdup increases down the column and average values of M and m can be used with average values of holdup. At high holdups the average drop size increases up the column and considerable mixing of the drops take place (*14*). Somewhat greater values of M and smaller values of m than in Figures 6 and 7 are recommended for this range in Table 2.

Five of the calculated temperature profiles, for different ratios of flow rates, holdup and direction of heat flow are shown in Figures 8 to 12 together with the experimental points. The agreement of the experimental and calculated temperature profiles is very good in all cases.

Table 2. Recommended Values of M and m for Calculation of the Temperature Profiles for Dispersed Packings

Average holdup in column	0.06	0.06 to 0.4	>0.4
M	1.0	0.83	0.83
m	0.023	0.03	0.023

Table 3. Effect of Variation of Parameters on the Accuracy of the Calculated Temperature Profiles.

Parameter	Change of parameter from calculation 1 to calculation 2 %	$100 \times \frac{t_{do1} - t_{do2}}{t_{di} - t_{do1}}$ %
M	10	2.5
m	10	2
z_b or z_d	10	2

Moderate variations of the values of M, m, z_b, and z_d have a small effect on the calculated temperature profiles. This is shown in Table 3 for $R = 1$.

For larger values of R variations of these four parameters have greater effect on the accuracy of the calculated temperature profiles.

Since this work was limited to narrow temperature ranges and dispersed packing of drops, the theoretical model was also tested for application to wider temperature ranges and for dense packings of drops by calculation of the temperatures at the top of the column for a few runs chosen at random from the studies, for which the flow rates, inlet, and outlet temperatures and in most cases

Table 4. Calculation of the Temperatures at the Top of the Columns of Four Different Studies by the Proposed Model.

Source	Garwin Smith (7)	Barbouteau (2)	Pierce et al (24)	Kehat Letan (13)
Number of run	2-39	5-2	Figure 5	1-16
Dispersed phase	Benzene	Gasoline	Mercury	Kerosene
Column diameter, cm.	5	40		7.5
Length of packing of drops, cm.	185	400	50	150
R	0.5	0.5	1.0¶	1.08
r	0.395	0.425	0.45	0.39
H	0.215	0.06 (est.)	<0.06	0.55‡
t_{di}	160.9°F.	118°C.	205°F.	62.3°C.
t_{co}	89.7°F.	29°C.	125°F.	41.3°C.
t_{do}	73.6°F.	15°C.	105°F.	29.0°C.
t_{ci}	73.5°F.	7°C.	80°F.	27.0°C.
z_b cm.	10	35	10†	0
z_d cm.	0	5		0
M	0.83	1.0	1.0	0.6§
m cm.$^{-1}$	0.03	0.023*	0.023	0.025§
t_{do} calc.	73.5°F.	7.4°C.	103.5°F.	30.1°C.
t_{ci} calc.	72.2°F.	5.5°C.	79.5°F.	28.7°C.
$\frac{t_{do}\text{ calc.} - t_{do}}{t_{di} - t_{do}} \times 100$ %	0.1	7.5	1.5	3.2
$\frac{t_{ci}\text{ calc.} - t_{ci}}{t_{co} - t_{ci}} \times 100$ %	7.5	6.8	1.1	12

In all cases the continuous liquid phase was water.
* Using $m = 0.01$ improves the accuracy of t_{do} calc. to 4.5%.
† Increasing $z_b + z_d$ to 30 cm. decreases the accuracy of t_{do} calc. to 14%.
‡ Dense packing of drops.
§ Using $M = 0.4$ and $m = 0.015$ improves the accuracy of t_{do} calc. to 1.4%.
¶ Calculated from a heat balance.

average holdup were given. The temperatures at the bottom of the column were used to calculate the temperatures at the top of the column for comparison with the experimental data. The parameters for the equations were taken from Tables 1 and 2 of this paper for the different liquids and drop sizes of the four studies analyzed in Table 4.

These parameters and the results of four such calculations are given in Table 4. Agreement of the calculated temperatures with the experimental temperatures is good and can be improved when more data about the effect of drop size and more information on M and m are available. The difference in the accuracy of the calculations for the two phases in two cases is due to the poor heat balance for these runs in the original studies.

The equations and numerical values of the parameters presented in this work can therefore be applied to other systems and wide temperature ranges.

CONCLUSIONS

The good agreement of the theoretical model with the experimental results shows that heat transfer in a spray column is controlled by the fluid dynamics of the system and not by the resistance to heat transfer inside or at the surface of the drops. Heat transfer coefficients or HTU should not be used for the correlation of experimental data in spray column heat exchangers. The use of mass transfer coefficients in extraction spray columns should be reviewed in the light of the results of this work.

The equations developed in this work can be used for the design of spray column heat exchangers.

It is planned to check the values obtained for M and m in this work by tracer studies in the near future.

ACKNOWLEDGMENT

This work is based on the D.Sc. thesis of Ruth Letan at the Technion, Israel Institute of Technology.

NOTATION

Cp = heat capacity cal./g. °C.
F = defined by Equation (33)
H = average holdup
l = length of wake shedding zone cm.
l' = length of drop packing extending into conical entry section cm.
M = ratio of wake to drop volumes = M_D/v_D
M_D = wake volume cc.
m = volume of wake elements shed per volume of drop and unit length of column cm.$^{-1}$
m_w = volume of wake shed cc.
P = $(1 + MR)/R$
R = V_d/V_c
r = $(\rho Cp)_d/(\rho Cp)_c$
S = defined by Equation (19)
t = temperature °C.
V_c = superficial velocity of continuous liquid cc./sq. cm. sec.
V_d = superficial velocity of dispersed liquid cc./sq. cm. sec.
v_D = volume of drop cc.
z = distance along column; length of zone cm.
α = defined by Equation (19) cm.$^{-1}$
ϵ = small value
θ = dimensionless temperature
ρ = density g./cc.

Subscripts

a = zone a; jump
b = zone b
c = continuous phase
d = dispersed phase; zone d
e = zone e
i = inlet
l = at top of wake shedding zone
l_1 = at inlet of continuous phase
o = outlet
s = at intermediate zone
w = wake
z = within wake shedding zone
1 = calculated from set of parameters
2 = calculated from another set of parameters

LITERATURE CITED

1. Allen, H. D., W. A. Kline, E. A. Lawrence, C. J. Arrowsmith, and C. Marsel, *Chem. Eng. Progr.*, **43**, 459 (1947).
2. Barbouteau, I., *Rev. Inst. Franc. Petrole*, **11**, 358 (1956).
3. Bauerle, G. L., and R. C. Ahlert, *Ind. Eng. Chem. Process Design Develop.*, **4**, 225 (1965).
4. Cavers, S. D., and J. E. Ewanchyna, *Can. J. Chem. Eng.*, **35**, 113 (1957).
5. Garner, F. H., *Trans. Inst. Chem. Engrs.*, **28**, 88 (1950).
6. ———, and M. Tayeban, *Anales Real Soc. Espan. Fis. Quim., Ser. B*, **56**, 479 (1960).
7. Garwin, L., and B. D. Smith, *Chem. Eng. Progr.*, **49**, 591 (1953).
8. Gier, T. E., and J. O. Hougen, *Ind. Eng. Chem.*, **45**, 1362 (1953).
9. Hashizume, M., H. Okamoto, and Y. Mokoko, *Kagaku Kogaku*, (English ed.) **3**, 125 (1965).
10. Heertjes, P. M., W. A. Holve, and H. Talsma, *Chem. Eng. Sci.*, **3**, 122 (1954).
11. Hendrix, C. D., S. B. Dave, and H. F. Johnson, Paper presented at AIChE. National Meeting, Memphis, Tenn. (Feb. 1963).
12. Johnson, A. I., G. W. Minard, C. J. Huang, J. H. Hansuld, and V. M. McNamara, *AIChE J.*, **3**, 101 (1957).
13. Kehat, E., and R. Letan, Paper presented at Israel National Council for Research and Development (Dec., 1963) (Hebrew text).
14. Letan, R., D.Sc. dissertation, Technion, Israel Institute of Technology, Haifa, Israel (1966) (Hebrew text).
15. Letan, R., and E. Kehat, Paper presented at Israel National Council for Research and Development (Dec., 1964).
16. Letan, R., and E. Kehat, *AIChE J.*, **11**, 804 (1965).
17. ———, *Chem. Eng. Sci.*, **20**, 856 (1965).
18. ———, *AIChE J.*, **13**, 443 (1967).
19. Magarvey, R. H., and R. L. Bishop, *Can. J. Phys.*, **3**, 1418 (1961).
20. ———, *Phys. Fluids*, **4**, 800 (1961).
21. Möller von, W., *Physik z.*, **39**, 57 (1938).
22. Nisi, H. and A. W. Porter, *Phil. Mag.*, **46**, 75 (1923).
23. Othmer D. F., R. F. Benenati, and G. C. Goulandris, *Chem. Eng. Progr.*, **59**, No. 12, 63 (1963).
24. Pierce, R. D., O. E. Dwyer, and J. J. Martin, *AIChE J.*, **5**, 257 (1959).
25. Rose, P. M., and R. C. Kintner, AIChE J., **12**, 530 (1966).
26. Rosenthal, H., M.Ch.E. thesis, New York Univ., New York (1949).
27. Sukhatme, S. P., and M. Hurwitz, *Office of Saline Water Progr. Rept.*, 120 (1964).
28. Sukhatme, S. P., M. Hurwitz, and S. E. Sadek, Paper presented at AIChE., National Meeting, Atlantic City, N. J. (Sept. 1966).
29. Taneda, S., *Rep. Res. Inst. Appl. Mech.* (Japan), **4**, 99 (1956).
30. Thompson, W. S., T. Woodward, W. A. Shrode, E. D. Baird, and D. A. Oliver, *Office of Saline Water Progr. Repts.*, 63 (1962), 78 (1963).
31. Thorsen, G., and S. G. Terjesen, *Chem. Eng. Sci.*, **17**, 137 (1962).
32. Woodward, T., *Chem. Eng. Progr.*, **57**, No. 1, 52 (1961).

Manuscript received April 20, 1967; revision received August 3, 1967; paper accepted August 7, 1967.